

Article

Comparative Study of the Characteristics and Activities of Pd/ γ -Al₂O₃ Catalysts Prepared by Vortex and Incipient Wetness Methods

Anil C. Banerjee ^{1,*},[†] , Kristina W. Golub ^{2,†} , Md. Abdul Hakim ¹ and Mehmet Z. Billor ³

¹ Department of Chemistry, Columbus State University, Columbus, GA 31907, USA; hakim_mdadbul@columbusstate.edu

² School of Chemical & Biomolecular Engineering, Georgia Institute of Technology, Atlanta, GA 30332, USA; kgolub@gatech.edu

³ Department of Geosciences, Auburn University, Auburn, AL 36849, USA; mzb0009@auburn.edu

* Correspondence: banerjee_anil@columbusstate.edu; Tel.: +1-706-569-3030

† Co-first authors.

Received: 19 February 2019; Accepted: 1 April 2019; Published: 4 April 2019



Abstract: 5 wt% Pd/ γ -Al₂O₃ catalysts were prepared by a modified Vortex Method (5-Pd-VM) and Incipient Wetness Method (5-Pd-IWM), and characterized by various techniques (Inductively coupled plasma atomic emission spectroscopy (ICP-AES), N₂-physisorption, pulse CO chemisorption, temperature programmed reduction (TPR), X-ray photoelectron spectroscopy (XPS), scanning transmission electron microscopy (STEM), and X-ray diffraction (XRD)) under identical conditions. Both catalysts had similar particle sizes and dispersions; the 5-Pd-VM catalyst had 0.5 wt% more Pd loading (4.6 wt%). The surfaces of both catalysts contained PdO and PdO_x with about 7% more PdO_x in 5-Pd-VM. High-angle annular dark-field scanning transmission electron microscopy (HAADF-STEM) and scanning electron microscope (SEM) images indicated presence of PdO/PdO_x nanocrystals (8–10 nm) on the surface of the support. Size distribution by STEM showed presence of smaller nanoparticles (2–5 nm) in 5-Pd-VM. This catalyst was more active in the lower temperature range of 275–325 °C and converted 90% methane at 325 °C. The 5-Pd-VM catalyst was also very stable after 72-hour stability test at 350 °C showing 100% methane conversion, and was relatively resistant to steam deactivation. Hydrogen TPR of 5-Pd-VM gave a reduction peak at 325 °C indicating weaker interactions of the oxidized Pd species with the support. It is hypothesized that smaller particle sizes, uniform particle distribution, and weaker PdO/PdO_x interactions with the support may contribute to the higher activity in 5-Pd-VM.

Keywords: methane combustion; PdO-PdO_x/ γ -Al₂O₃ catalyst; vortex method; catalytic activity; steam deactivation; 72-h stability test, metal-support interaction

1. Introduction

Catalytic combustion of methane at low temperatures has been a challenging issue both academically and industrially. Since 2010 more than 5000 articles have been published each year on methane combustion [1]. Heterogeneous catalysts including noble metal-based catalysts on various supports have been found to be an effective route for methane oxidation [1,2]. Two recent reviews reported several articles claiming success with palladium catalysts on various supports [1,3]. Among the supported palladium catalysts, gamma alumina (γ -Al₂O₃) has received more attention [4–9]. Banerjee et al. [4] developed a PdO-PdO_x/ γ -Al₂O₃ catalyst by a novel Vortex Method which showed high activity with methane conversion of 90–94% at 300–320 °C. A Pd catalyst on phosphorous-doped mesoporous γ -Al₂O₃ support achieved total methane combustion at 345 °C [5]. Gorte et al. [6] prepared

a catalyst with ZrO_2 coating on $\text{Pd}/\gamma\text{-Al}_2\text{O}_3$ by atomic layer adsorption which exhibited high activity at 212 °C. Several researchers [7–9] reported $\text{Pd}/\gamma\text{-Al}_2\text{O}_3$ catalysts with methane conversion of 30–90% at 320–400 °C.

Several Pd catalysts have also been developed using other supports. Liu et al [10] developed a rice husk derived porous silica support for a Pd-CeO_2 catalyst for low temperature combustion of methane with 90% conversion at 325 °C. A monolithic $\text{Pd}/\text{Al}_2\text{O}_3/\text{Fe-Ni}$ catalyst with metal foam as matrix in a microcombustor improved methane conversion to more than 99% [11]. Cargnello et al. [12] developed a novel $\text{Pd@CeO}_2/\text{hydrophobic-Al}_2\text{O}_3$ core-shell catalyst that had methane conversions of 50% and 100% at 325 °C and 400 °C respectively. A Pd/Ceria nanocatalyst on Al_2O_3 support was prepared by solution combustion method with 90% methane conversion at 400 °C [13]. A nanozeolite silicalite-1 coated cordierite catalyst and a nitrogen-modified perovskite-type composite catalyst eliminated 90% methane at 350 °C [14,15]. A $\text{Pd}/\text{Co}_3\text{O}_4$ catalyst on ZrO_2 open cell foam converted about 90% methane at 325 °C and 100% at 400 °C [16]. Zhang et al. [17] prepared a Pd catalyst on $\text{Al}_2\text{O}_3\text{-CeO}_2$ support that converted 80% methane at 320 °C and 100% at 400 °C. A 1 wt% Pd catalyst with 10 wt% TiO_2 on mesoporous silica support converted almost 100% methane at 350 °C [18]. Liotta et al. [19] prepared a mesoporous silica supported Pd (1 wt%)/ $\text{LaMn}_{0.4}\text{Fe}_{0.6}\text{O}_3$ catalyst that exhibited 60% conversion in the presence of 10 ppm SO_2 . Ma et al. [20] developed a Pd/CeO_2 catalyst by impregnation method with hydrazine hydrate reduction; the catalyst eliminated 90% methane at 336 °C. Martin et al. [21] reported the development of a $\text{Pd}/\text{Co}_3\text{O}_4$ catalyst with 100% methane conversion at 360 °C in a gas feed of 1% CH_4 , 18% O_2 , and balance N_2 .

The activity and stability of Pd catalysts depend on preparation methods, particle size distribution, morphology, oxidation states, structure, and support interactions [1,3,22]. Additional concerns with $\text{Pd}/\text{Al}_2\text{O}_3$ catalysts have been deactivation by water and long-term stability [7,12,22]. We previously reported the development of a $\text{PdO-PdO}_x/\gamma\text{-Al}_2\text{O}_3$ catalyst by vortex method [4] and the catalyst showed low-temperature activity for methane combustion. As a continuation of this project, we modified the procedure of catalyst preparation by vortex method and planned to compare the properties and activity of the modified catalyst with a $\text{Pd}/\gamma\text{-Al}_2\text{O}_3$ catalyst prepared by Incipient Wetness Method [23] under identical experimental conditions. We also conducted long-term stability tests and effect of water and nitrogen in the gas feed with both catalysts to test their performance.

2. Results

2.1. Catalyst Preparation

Catalysts were prepared by a modified Vortex Method (VM) [4] and Incipient Wetness Method (IWM) [5,23] assuming a 5.0 wt% Pd loading on $\gamma\text{-Al}_2\text{O}_3$ support. The total mixing time in the original Vortex Method [4] was modified to match with the Incipient Wetness method. The details of the methods of preparation are given in the methods section. In this research article the catalysts prepared by VM and IWM are designated as 5-Pd-VM and 5-Pd-IWM respectively. Since the preparation method was modified, the properties, and characterization data by X-ray photoelectron spectroscopy (XPS) and scanning transmission electron microscopy (STEM) of the 5-Pd-VM catalyst differ from the original catalyst reported earlier [4] probably due to changes in preparation methods, crystallite size, particle size distribution, morphology, oxidation states, structure, and support interactions [1,3,5,6,22]. While the properties of the original catalyst changed, the activity for methane combustion remained almost the same. We do not fully understand at this stage why and how some of the catalyst properties of the original VM catalyst changed even though the activity remained almost the same.

2.2. Catalyst Characterization

2.2.1. Pulse CO Chemisorption

CO pulse chemisorption experiments provided measures of the dispersion and particle size (crystallite size) of the catalyst. The calculations were done based on actual Pd weight percent measured by Inductively Coupled Plasma Atomic Emission Spectrometry (ICP-AES) and assuming a 1:1 ratio of CO to Pd on the surface. The 5-Pd-VM catalyst had a slightly lower dispersion and a larger metal nanoparticle diameter compared to the 5-Pd-IWM catalyst. Both catalysts were made of nanoparticles in the range of 8.6–8.9 nm. However, 5-Pd-VM appeared to have a higher metallic surface area, although this could be attributed to having a slightly higher Pd wt%. The dispersion and particle sizes of the catalysts were similar to the data reported in the literature for Pd/ γ -Al₂O₃ catalysts [8,9].

2.2.2. Inductively Coupled Plasma Atomic Emission Spectrometry (ICP-AES)

Although both catalysts had a target of 5.0 wt% Pd loading on γ -Al₂O₃ support, it appears there was slightly more Pd in 5-Pd-VM (4.58 wt% Pd) compared to 5-Pd-IWM (4.06 wt% Pd). This indicates that vortex mixing was a relatively better method in retaining Pd in the sample. Table 1 summarizes the physical and chemical properties of the catalysts. The properties were similar in both catalysts.

Table 1. Properties of the catalysts.

Properties	Values	
	5-Pd-VM	5-Pd-IWM
Targeted Wt% Pd	5.0%	5.0%
Pd Wt% [ICP-AES]	4.6%	4.1%
Surface Area *	127 m ² /g	129 m ² /g
CO uptake in chemisorption	54.4 μ mol/g	49.9 μ mol/g
Dispersion	12.6%	13.1%
Metal Surface Area	2.6 m ² /g	2.4 m ² /g
Nanoparticle diameter (hemisphere)	8.9 nm	8.6 nm

* From BET (Brunauer, Emmett and Teller) method.

2.2.3. X-ray Photoelectron Spectroscopy (XPS)

Ex-situ XPS was used to identify near-surface species and compositions of the catalysts 5-Pd-VM and 5-Pd-IWM pre- and post-reaction. The results are shown in Figures 1 and 2 and Table 2. Survey spectra obtained in the Pd 3d, O 1s, and Al 2p regions confirmed the relative presence and oxidation states of each element. Pd 3d spectra suggested that the nanoparticles in both catalysts were in oxidized states, with deconvoluted Pd 3d_{5/2} binding energy (BE) peaks at 335.8 and 336.9 eV representing PdO_x (palladium native oxide PdNtv or palladium nonstoichiometric oxide) and PdO species, respectively [24]. Deconvolution of these surface species showed that 5-Pd-VM had about ~7% more of PdO_x and ~7% less PdO compared to the catalyst 5-Pd-IWM. XPS data also confirmed the absence of metallic Pd (BE, 335.3 eV) in both catalysts [24,25]. The absence of metallic Pd in both catalysts is due to lower calcination temperature of 500 °C and decomposition temperature of PdO is higher than 700 °C [25]. Our results are contrary to previous studies which report the presence of Pd in such catalysts [23,26–28]. XPS data were also collected for the two catalysts after reaction with 1% methane, 4% oxygen and balance helium at 450 °C for 24 h. There was no significant change in the relative amounts of PdO and PdO_x after reaction (Figure 1b,d).

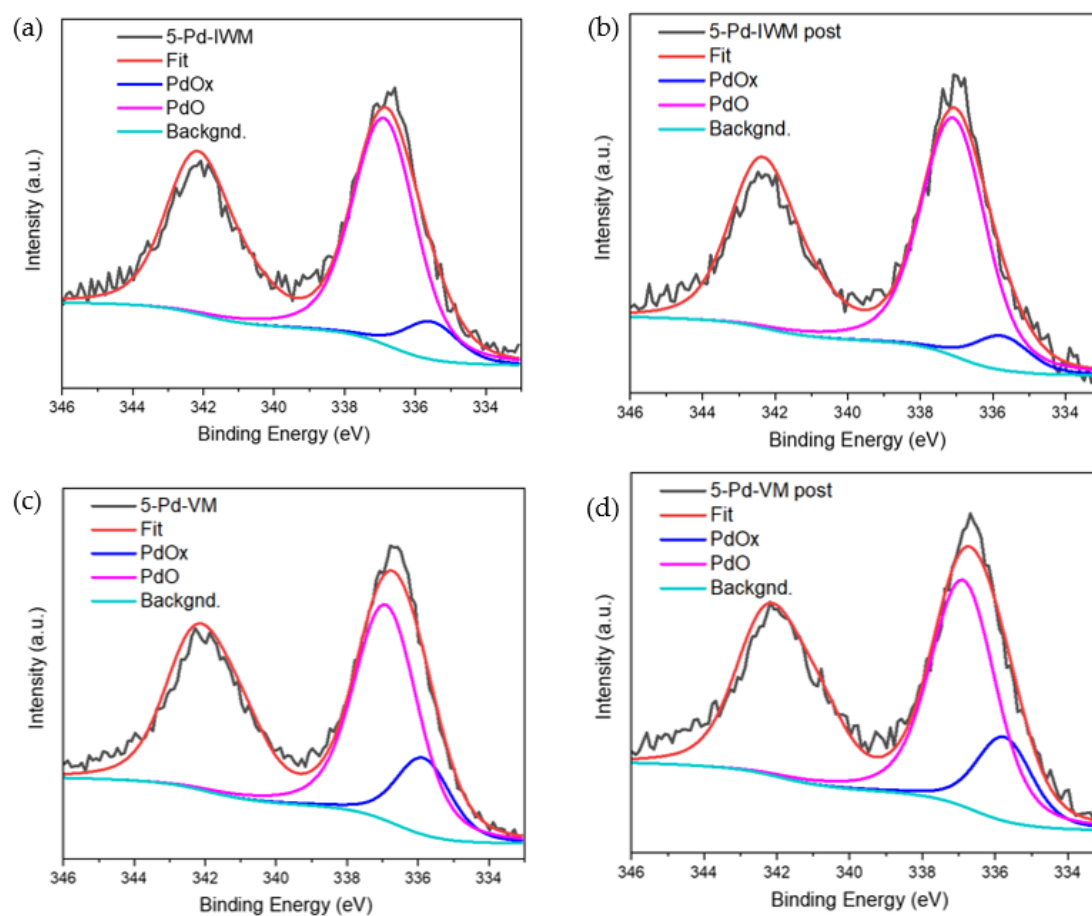


Figure 1. XPS deconvolution of pre- and post-reaction; 5-Pd-IWM (a,b) and 5-Pd-VM (c,d) in the Pd3d binding energy region.

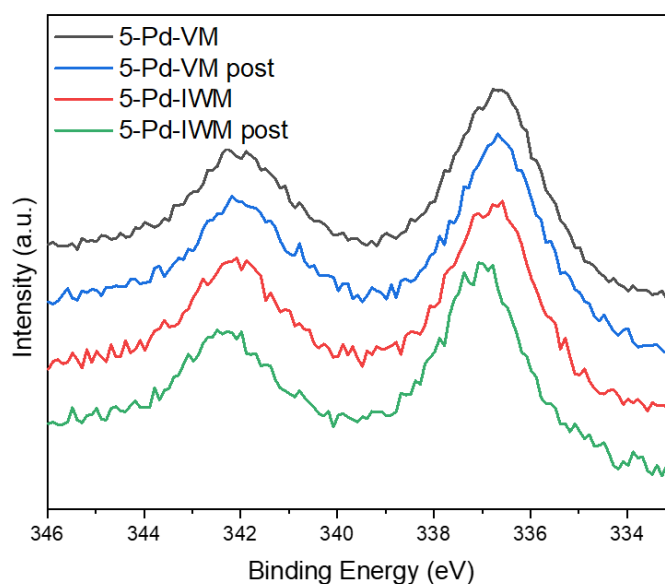


Figure 2. XPS of 5-Pd-VM and 5-Pd-IWM catalysts pre- and post-reaction in the Pd3d binding energy region.

Table 2. XPS deconvolution of catalysts pre- and post-reaction in Pd 3d_{5/2} region. VM: Vortex Method; IWM: Incipient Wetness Method.

Sample	PdO _x (Atomic %)	PdO (Atomic %)
5-Pd-VM	23	77
5-Pd-VM Post	24	76
5-Pd-IWM	16	84
5-Pd-IWM Post	11	89

2.2.4. Scanning Transmission Electron Microscopy (STEM)

High-angle annular dark field scanning transmission electron microscopy (HAADF-STEM) images (Figures 3 and 4) identified PdO/PdO_x in nanoparticle sizes. Both catalysts contained nanoparticles with an average PdO/PdO_x crystallite size of 8.5 nm in 5-Pd-VM and 9.8 nm in 5-Pd-IWM catalysts. The average particle sizes of our nanocatalysts (~10 nm) are similar to the data reported by other researchers [8,29].

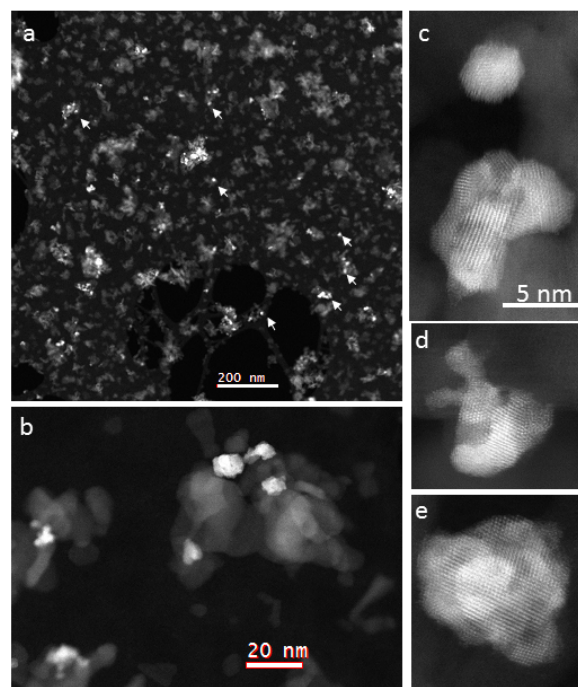


Figure 3. (a,b) Low-magnification high-angle annular dark field scanning transmission electron microscopy (HAADF-STEM) image of 5-Pd-VM catalyst. The tiny bright dots are PdO/PdO_x nanoparticles; some are pointed by arrowheads. (c–e) high magnification HAADF STEM images to show the crystal structure of PdO/PdO_x clusters.

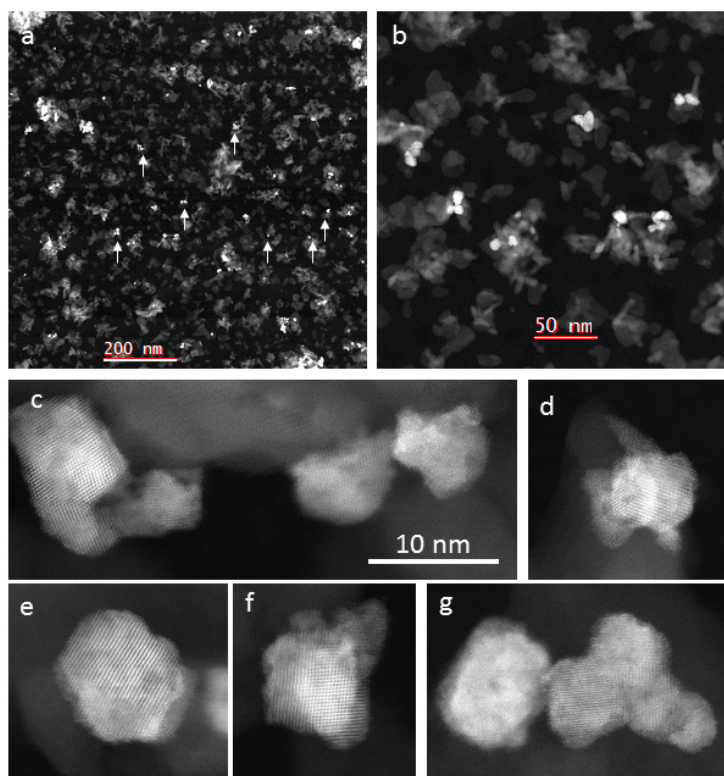


Figure 4. (a,b) Low-magnification HAADF-STEM image of 5-Pd-IWM catalyst. The tiny bright dots are PdO/PdO_x nanoparticles; some are pointed by arrowheads. (c–g) High magnification HAADF-STEM images to show the crystal structure of of PdO/PdO_x clusters.

Figure 5 shows the particle size distribution in the two catalysts based on HAADF-STEM data. The size distributions are somewhat different in the two catalysts:

- (i) The crystallite sizes are 3–13 nm in 5-Pd-VM and 3–17 nm in 5-Pd-IWM;
- (ii) The catalyst 5-Pd-VM contains more smaller particles 3–5 nm than 5-Pd-IWM;
- (iii) The catalyst 5-Pd-IWM contains bigger particles 15–17 nm and these are absent in 5-Pd-VM;
- (iv) The particle size distribution was narrower (2–14 nm) in 5-Pd-VM than 5-Pd-IWM (2–18 nm).

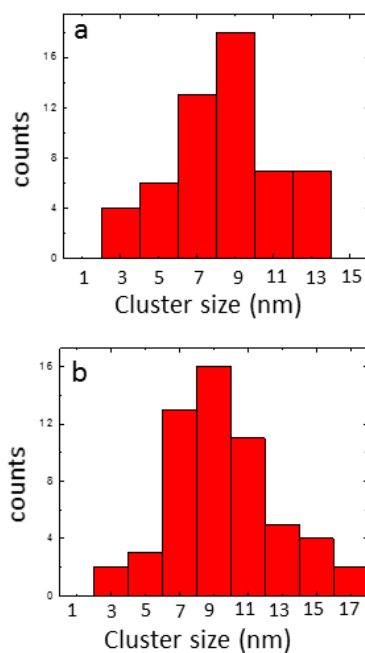


Figure 5. Size distribution of PdO/PdO_x particles in (a) 5-Pd-VM and (b) 5-Pd-IWM.

In order to determine whether the metal oxide nanoparticles were on the surface of the support or embedded, the HAADF-STEM and scanning electron microscopy (SEM) images were analyzed further. Figure 6 gives the HAADF and SEM images for the two catalysts. The bright particles of PdO/PdO_x are on the surface of the support and not embedded in the support as shown in the SEM images.

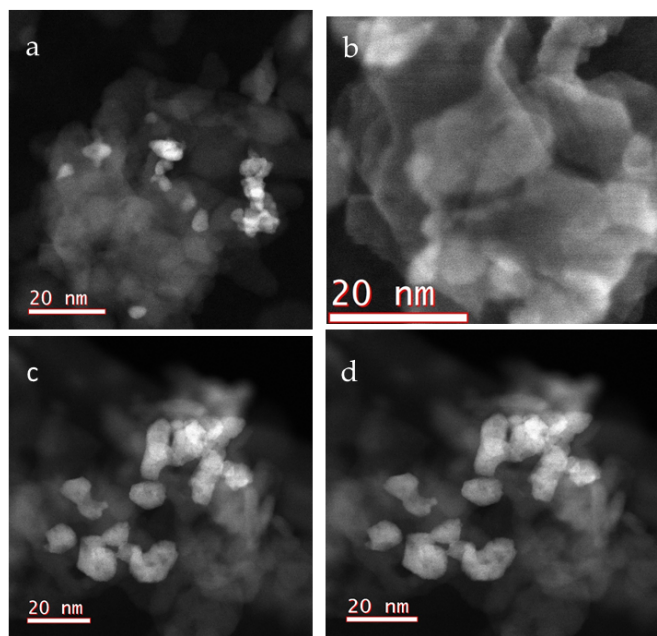


Figure 6. HAADF-STEM and SEM images. (a) HAADF-STEM image of 5-Pd-VM; (b) SEM image of 5-Pd-VM from the same area; (c) HAADF-STEM image of 5-Pd-IWM; (d) SEM image of 5-Pd-IWM from the same area. The bright particles of PdO/PdO_x are on the surface of the support as showing in the SEM image.

2.2.5. Temperature Programmed Reduction

Hydrogen temperature programmed reduction (TPR) results are shown in Figure 7. The 5-Pd-IWM catalyst prepared by IWM showed hydrogen consumption at 215–675 °C with a peak at 375 °C. The

catalyst 5-Pd-VM had hydrogen consumption at 190–625 °C with a peak at 325 °C. This indicates that the oxidized species (PdO/PdO_x) in 5-Pd-VM tends to be reduced at slightly lower temperatures than the same catalyst prepared by IWM. In the TPR experiment, the last step in the pretreatment involved cooling the catalyst to below 50 °C in a flow of H₂/He; during this pretreatment, it was possible for some of the PdO/PdO_x species on the surface to be reduced by hydrogen to produce metallic Pd which then adsorbed hydrogen. The negative endothermic peak at around 70 °C was due to desorption of hydrogen on the metallic surface of Pd that was adsorbed at room temperature [30] or due to decomposition of palladium hydride [23]. CH₄-TPR of Pd catalysts on Al₂O₃, MgO, and ZrO₂ supports showed a peak at 500 °C for the Pd/Al₂O₃ catalyst and the peak temperature was slightly lower compared to the other two catalysts. This indicated that the PdO oxidized species were more reactive on the Al₂O₃ support due to less metal-support interactions [9]. Chen et al. [5] did hydrogen TPR of a Pd catalyst on phosphorous-doped mesoporous alumina and observed a broad peak at 250–560 °C that was assigned to the reduction of the PdO species that strongly interacted with the support. It appears from the TPR data that the PdO species had less interaction with the support in the 5-Pd-VM catalyst and that could have contributed to the higher activity compared to the 5-Pd-IWM catalyst.

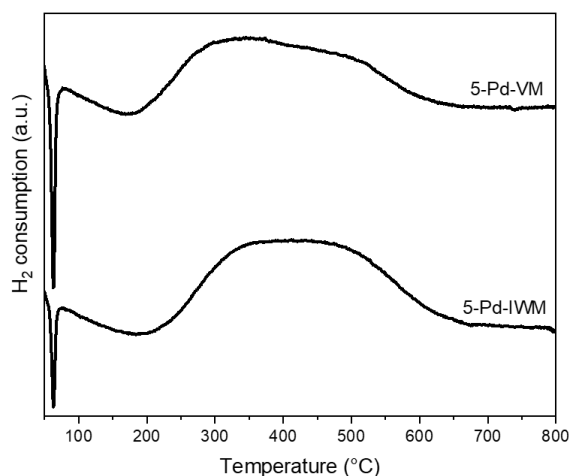


Figure 7. H₂-TPR of catalyst 5-Pd-IWM and 5-Pd-VM.

2.2.6. X-ray Diffraction

The X-ray diffraction (XRD) data of the catalysts 5-Pd-VM and 5-Pd-IWM, γ -Al₂O₃ and PdO are given in Figure 8.

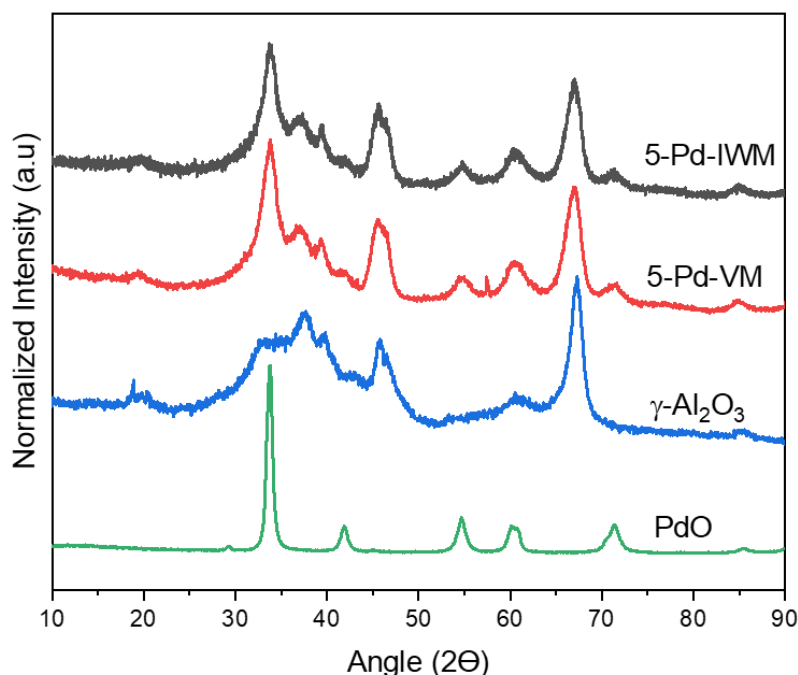


Figure 8. X-ray diffraction data.

The strong peaks for γ - Al_2O_3 are at 46° and 67.4° and the identifying peak for PdO is a strong peak at 34.1° . Both catalysts produced three main peaks at 34.1° , 46° and 67.4° , confirming the presence of PdO and γ - Al_2O_3 and no Pd metal (XRD peaks 39° , 49° , 82°). The XRD data confirmed that PdO and γ - Al_2O_3 in both catalysts were crystalline [5]. Our XRD data were similar to those reported in the literature [8,9].

2.3. Activity Studies

2.3.1. Conversion of Methane in 1–2% Methane, 4% Oxygen, Balance Helium Gas Feed

The gas hourly space velocity (GHSV) is one factor that affects methane conversion [5]. To assess the effect of GHSV on conversion, runs were conducted at five flow rates in the range 50–200 cc/min at laboratory ambient temperature and pressure and using 0.2 g 5-Pd-VM catalyst, reaction bed temperature 265°C and reaction period of 20 min. The GHSV was 15,000–60,000 cc.g.cat $^{-1}$.h $^{-1}$. The conversions remained constant at 25% in the GHSV range, 37,000–60,000 cc.g.cat $^{-1}$.h $^{-1}$. Under these conditions, the catalytic reaction was kinetically controlled and not diffusion controlled. Hence, for all subsequent activity runs a GHSV of 45,000 cc.g.cat $^{-1}$.h $^{-1}$ was selected. Each activity run was conducted in a fixed bed differential flow reactor at a fixed temperature for a period of 20 min with 0.2 g catalyst in the fixed bed and a flow rate of 150 cc/min. The activities of the two catalysts (5-Pd-VM and 5-Pd-IWM) were measured by calculating conversions of methane at different temperatures in the range 250–350 $^\circ\text{C}$. A pre-mixed gas of 1% methane, 4% oxygen, and balance helium was used in the feed to represent a “lean-burn” condition (oxygen rich); a second gas mixture of 2% methane, 4% oxygen and balance helium was used to represent an ideal stoichiometric ratio for the catalytic combustion. Figure 9 gives the conversions of methane by the two catalysts at different temperatures.

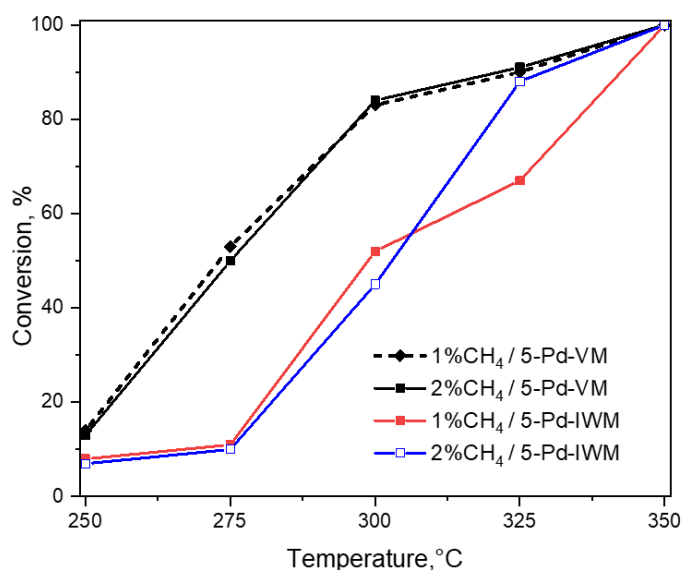


Figure 9. Activities of the 5-Pd-VM and 5-Pd-IWM catalysts at different temperatures and either 1% or 2% methane gas feed (GHSV = 45,000 cc.g.cat⁻¹.h⁻¹/g_{cat}/h; reaction period = 20 min).

The conversion-temperature data provided some important conclusions about the activities of two catalysts:

- (i) The catalyst 5-Pd-VM showed higher activity at 275 °C compared to the catalyst 5-Pd-IWM which gave very low activity at this temperature with both 1% and 2% methane in the feed; the trends were similar at 300 °C, with 85% conversion by 5-Pd-VM and about 50% by 5-Pd-IWM.
- (ii) Catalyst 5-Pd-VM produced a high conversion of 90% methane at 325 °C for both 1% and 2% methane in the gas feed, while the conversions at this temperature for 5-Pd-IWM were much lower (67%) with 1% methane and about 88% with the 2% methane in the gas feed.
- (iii) Both catalysts converted 100% methane at 350 °C under both lean and stoichiometric conditions.

The catalyst reported in a previous publication [4] showed a decreasing trend in conversion in the temperature range of 330–400 °C and GHSV of 300,000 cc.g.cat⁻¹.h⁻¹ (0.2 g catalyst bed and flow rate of 1000 cc/min of mixed gas at normal laboratory temperature). However, in the present study we did not see this trend and the conversion increased and reached 100% at 350 °C with the GHSV maintained at 45,000 cc.g.cat⁻¹.h⁻¹ (0.2 g catalyst bed and flow rate of 150 cc/min of mixed gas at room temperature). It appears that a seven-fold decrease in GHSV and thereby a seven-time increase in the contact time was a major factor for the increase in conversion. However, the reaction was not diffusion-controlled in this range of space velocity and particles size of the activity experiments. Similar trends on the increase of catalytic activity with decrease in GHSV have also been reported [5,31,32].

The Pd/γ-Al₂O₃ catalysts reported by previous researchers exhibited low activities (30–50%) for methane combustion at 325 °C [7–9]. However, our catalyst 5-Pd-VM showed much higher activity at this temperature. These activity results indicate that the Vortex Method (VM) is a better technique for catalyst preparation than IWM. The high activities exhibited by the Pd/γ-Al₂O₃ catalyst prepared by Vortex method are similar to catalysts developed by other techniques [12,14,16,31,33,34].

2.3.2. Conversion of Methane in 1% Methane, 4% Oxygen, and Balance Nitrogen Gas Feed

The activities of the catalysts 5-Pd-VM and 5-Pd-IWM were determined experimentally by passing 150 cc of a mixed gas containing 1% methane, 4% oxygen and balance nitrogen over a 0.2 g catalyst bed for 20 min at 275–325 °C. Table 3 gives the conversion of methane at different temperatures for the two catalysts. A comparison of the activities (Figure 9 and Table 3) shows that both catalysts improved performance in the presence nitrogen compared to the mixed gas containing helium. However, at

lower temperatures 250–275 °C the catalyst 5-Pd-VM exhibited much higher activity than 5-Pd-IWM; but catalyst 5-Pd-IWM had a significant improvement in activity at 300 °C. Simplicio et al. [8] reported similar low catalytic activities for Pd/ γ -Al₂O₃ catalysts prepared by Incipient Wetness Method (IWM) in the presence of 0.5% CH₄, 2% O₂ and balance N₂.

Table 3. Activities of catalysts in 1% methane, 4% oxygen, balance nitrogen.

Temperature, °C	Methane Conversion, %	
	5-Pd-VM	5-Pd-IWM
250	61	18
275	100	46
300	100	100

GHSV = 45,000 cc.g.cat⁻¹.h⁻¹; reaction period = 20 min.

The combustion of methane in both mixed gases (1.0% methane, 4.0% oxygen, balance helium and 1.0% methane, 4.0% oxygen and balance nitrogen) produced carbon dioxide and water as the products. We did not find carbon monoxide in the product gas mixtures in any of the runs. The mol % of carbon dioxide produced matched with the mol % CH₄ converted and this accounted for the carbon balance. We do not know why nitrogen in the gas feed improved the catalytic activities of both catalysts and particularly for the 5-Pd-VM catalyst at the lower temperature range.

2.4. Long-Term Stability Test of the Catalysts

Both catalysts were subjected to long-term stability tests by passing a mixed gas feed of 1.0% methane, 4.0% oxygen and balance helium over the catalysts separately in a fixed bed catalytic reactor at a selected temperature and GHSV of 45,000 cc.g.cat⁻¹.h⁻¹. The temperatures (T₂₅ and T₁₀₀) corresponding to 25% and 100 % conversions for the two catalysts as shown in Figure 9 were selected for the stability tests. The T₂₅ temperatures for 5-Pd-VM and 5-Pd-IWM catalyst were 265 °C and 288 °C respectively; the corresponding value for T₁₀₀ were 350 °C for both catalysts. The conversions of methane were calculated after 24 h, 48 h and 72 h for each catalyst. The data are given in Table 4. The methane conversions for 5-Pd-VM catalyst remained almost constant at 265 °C and 350 °C after 72 h. However, the activities of the catalyst 5-Pd-IWM decreased significantly at both T₂₅ and T₁₀₀ during 24–72 h stability tests. The results showed that the catalyst 5-Pd-VM was stable even after reaction with the gas feed for 72 h [5]. Similar long-term stability was displayed by Pd catalyst on other supports [16,21]. However, the catalyst 5-Pd-IWM deactivated after 24 h as reported by other researchers.

Table 4. Long-term stability tests of catalysts.

Reaction Period, h	Methane Conversion, %			
	5-Pd-VM		5-Pd-IWM	
	T ₂₅	T ₁₀₀	T ₂₅	T ₁₀₀
24	25	100	18	76
48	24	100	15	75
72	23	100	10	67

GHSV = 45,000 cc.g.cat⁻¹.h⁻¹; T₂₅ = 265 °C and T₁₀₀ = 350 °C for 5-Pd-VM; T₂₅ = 288 °C and T₁₀₀ = 350 °C for 5-Pd-IWM.

2.5. Effect of Steam

The conversions with catalyst 5-Pd-VM in the presence of steam were 89% after 2 h and 87% after 4 h at 350 °C. Under similar conditions, the conversions with catalyst 5-Pd-IWM were 78% and 71% respectively for 2 h and 4 h runs. The conversion of methane in the absence of steam in the feed for the

catalyst 5-Pd-VM after a 4 h run at 350 °C was 100%. This indicated that the catalyst 5-Pd-VM was relatively stable in the presence of steam after reaction for 4 h. Deactivation by steam has been reported as a major issue for supported Pd catalysts [12,22,32,35–37] particularly at temperatures above 325 °C. Steam deactivation in Pd/ γ -Al₂O₃ catalysts has been attributed to the reaction of PdO by steam to produce hydroxides [36,37]. However, our results show that the catalyst 5-Pd-VM prepared by Vortex method was comparatively stable in the presence of steam. A Pd catalyst on phosphorous-doped mesoporous γ -Al₂O₃ support showed good resistance to steam deactivation [5]. Some researchers also found Pt/Pd bimetallic catalysts to be resistant to steam during methane combustion due to diminished presence of surface hydroxyl groups [7,37].

2.6. Active Phases and Tentative Mechanism

The active phases of catalysts in methane combustion is still under dispute. Several authors had suggested PdO to be the active phase [2,7,12,33,38], while some suggested Pd to be the active phase [26,27,38]. Some researchers [2,4,7,29,39,40] have provided evidences for the existence of PdO_x as an active phase during the catalytic combustion of methane. Both catalysts contain PdO_x and PdO on the surface and no metallic Pd. Hence, it appears PdO/PdO_x may be the active phase in these two catalysts for methane combustion.

Both catalysts have similar dispersions and nanoparticle sizes; catalyst 5-Pd-VM had about 7% more PdO_x on the surface and about 0.5% more Pd content compared to 5-Pd-IWM catalyst. However, these properties alone cannot explain the higher activity of 5-Pd-VM catalyst. The catalyst 5-Pd-VM showed some unique characteristics compared to the 5-Pd-IWM catalyst:

- (i) The catalyst 5-Pd-VM contains more smaller particles 3–5 nm than 5-Pd-IWM (Figure 5).
- (ii) The particle size distribution was narrower (2–14 nm) in 5-Pd-VM than 5-Pd-IWM (2–18 nm) as shown in (Figure 5).
- (iii) PdO/PdO_x in 5-Pd-VM tends to be reduced at lower temperatures indicating the interaction between PdO species and the support was comparatively weaker (TPR results in Figure 7).

It seems these characteristics along with slightly higher Pd content and PdO_x may be contributing for the higher catalytic activity of the catalyst 5-Pd-VM. This explanation is supported by several recent publications [5,6,22]. Jiang et al. [5] argued that PdO support interactions was a major factor for the catalytic activity in methane combustion; Gorte et al. [6] found that the methane oxidation rate was dependent on Pd crystallite size and presence of hydroxyl groups on the surface of γ -Al₂O₃; Lundgren et al. [22] suggested that the activity of supported Pd nanocatalysts was sensitive to morphology, support, and pretreatment. The support alumina could also stabilize the PdO/PdO_x species and facilitate oxygen migration on the surface and from the bulk [23,29]. It is still not clear why the activity of the 5-Pd-VM catalyst prepared by Vortex Method is higher. Detailed investigations of the support before and after the catalytic reaction using small and wide angle XRD, STEM, BET, pore-volume and pore-size distribution [5], and in-situ X-ray absorption near edge structure (XANES) and extended X-ray absorption fine structure (EXAFS) [22] experiments would provide further evidence to elucidate the mechanism of catalytic combustion reaction of methane.

3. Materials and Methods

3.1. Catalyst Synthesis

The catalyst 5-Pd-IWM was prepared by Incipient Wetness Method (IWM). The precursor, an aqueous solution of palladium nitrate hydrate (Sigma-Aldrich, MO, USA) was added in 20- μ L installments to the solid support, γ -Al₂O₃ (Sigma-Aldrich, MO, USA) taken in a beaker and the mixture was stirred slowly until a dough-like consistency was formed. The total time for adding the precursor solution and mixing was 1 h. The catalyst was dried in an oven at 103 °C overnight and then calcined

at 500 °C for 6 h. The calcined catalyst was powdered and then sieved. The particles between 63–75 µm were selected for characterization and activity experiments.

The catalyst 5-Pd-VM was prepared by a modified Vortex Method described in a previous publication [4]. The total mixing time in the modified method was reduced to 1 h in order to be consistent with the IWM total mixing time. In the original Vortex method, vortexing was continued for additional 2 h after the precursor solution was completely transferred to the support. This modification was done to ensure that the only difference in the two methods was the mixing technique. The vortexing equipment consisted of a single tube holder and analog vortex mixer (Fisher Scientific; Catalog number 02-215-430, Asheville, NC, USA). The precursor, an aqueous solution of palladium nitrate hydrate (Sigma-Aldrich, MO, USA) was added in 20 µL installments to the solid support, γ -Al₂O₃ (Sigma-Aldrich, MO, USA) taken in a vortex tube attached to the tube holder. The mixture of the precursor solution and support was mixed by vortexing at 900 rpm in the vortex mixer for a total time of 1 h. The catalyst was dried in an oven at 103 °C overnight and then calcinated at 500 °C for 6 h. The calcined catalyst was powdered and then sieved. The particles between 63–75 µm were selected for characterization and activity experiments.

3.2. Catalyst Characterization

3.2.1. ICP-AES

Elemental analysis of Pd was conducted at Galbraith Laboratories, Inc., utilizing inductively coupled plasma atomic emission spectrometry (ICP-AES) by Perkin Elmer 5300V (Akron, OH, USA) after the samples were acidified or digested.

3.2.2. XPS

X-ray photoelectron spectroscopy (XPS) analysis was conducted using a Thermo K-Alpha spectrometer (ThermoFisher Scientific, Waltham, MA, USA) employing a monochromatic Al K α source with a double-focusing hemispherical analyzer. High-resolution spectra were taken of Pd2p, O1s, and C1s at a 0.1 eV step size, 50 ms dwell time, 50 eV pass energy, and a 400-µm spot size. The pressure inside the analytical chamber was approximately 5×10^{-8} torr. Charge referencing was done against adventitious carbon (C1s 284.8 eV).

3.2.3. Chemisorption and Physisorption

Chemisorption experiments including temperature programmed reduction (TPR) and pulse CO chemisorption were conducted in Micromeritics AutoChem II 2920 (Micromeritics Corporation, Norcross, GA, USA) [41]. Pd dispersion and metal particle size were measured with pulse chemisorption using CO as the probe gas. The catalyst (50 mg) was first pretreated in 20 mL/min of He (Airgas, PA, USA) at 200 °C for 2 h to remove preadsorbed species. The sample was then cooled to 50 °C and 20 mL/min of 10% H₂/He was passed over the sample. Next, the catalyst was reduced under a flow of 10% H₂/He and 450 °C at 5 °C/min and held for 1 h. The sample was then cooled to 300 °C in He flow for 30 min to remove adsorbed species. Afterwards, the sample was cooled to 30 °C to begin pulse CO testing. Doses of 10% CO/He (Airgas, PA, USA) were passed over the sample and analyzed in the TCD. Once saturation was reached, He was flowed over the sample for 60 min to remove physisorbed species. Finally, a second round of pulses was conducted to verify if there were any physisorbed species adsorbed. Dispersion and particle size (crystallite size) of the catalysts were calculated from the CO uptake, wt% of Pd from ICP analysis, and assuming a 1:1 ratio between the CO-adsorbed and Pd-active site.

For H₂-TPR, the catalyst (50 mg) was pretreated in 20 mL/min of He (UHP, Airgas, PA, USA) at 200 °C for 2 h, and then cooled to 50 °C in a 20 mL/min flow of 10% H₂/He. Next, the catalyst was reduced by ramping the furnace to 800 °C at a ramp rate of 5 °C/min under a flow of 10% H₂/He. After

passing through a liquid acetone/nitrogen trap, the gas flow was fed through a thermal conductivity detector (TCD) to determine hydrogen uptake.

Nitrogen physisorption was performed in a Quantachrome Quadrasorb SI volumetric analyzer (Quantachrome Instruments, Boynton Beach, FL, USA) at 77 K after the sample (50–100 mg) was pretreated at 110 °C under vacuum for 12 h. The surface area was estimated using the BET method following criteria outlined by Walton et al. [42] in the relative pressure range (P/P_0) of 0.005–0.03.

3.2.4. STEM

Scanning transmission electron microscopy (STEM) imaging was carried out on samples prepared on a lacey carbon-coated Au grid. HAADF-STEM images were collected in an aberration-corrected Hitachi HD2700 (Hitachi Ltd., Tokyo, Japan).

3.2.5. XRD

XRD data were collected at 25 °C by Bruker D2 Phaser Table top diffractometer (Bruker, Madison, WI, USA) using Cu-K α radiation 30 kV and 10 mA with step size 0.02 (2θ), step size 0.5 sec. between 10–90° (2θ).

3.3. Activity Measurements

Activity studies were conducted in a temperature-controlled horizontal tubular fixed-bed quartz reactor (internal diameter 12 mm). Catalyst (0.2 g) was packed in the fixed bed, supported by quartz wool and quartz beads to control the bed temperature of the exothermic combustion reaction. Particles between 63–75 μm were used in the activity experiments. Helium gas (150 cc/min) was passed through the catalyst bed and the reactor was heated by a temperature-controlled tubular furnace until a desired and constant temperature was achieved. The flow of helium was stopped and a certified gas mixture (Airgas, PA, USA) containing methane, oxygen, and balance helium or nitrogen was passed through an automatic mass flow controller (Aalborg, Orangeburg, NY, USA) and then to the catalyst bed. The effluent gas mixture (carbon dioxide, water vapor, unreacted methane, oxygen, and helium/nitrogen) was dried by passing through a moisture trap and then collected in a gas-tight syringe. A 1.0 cc sample of the sampled effluent gas mixture was injected into a gas chromatograph (GC Model 310, SRI Instruments, Torrance, CA, USA) fitted with a 6 ft. ShinCarbon (Restek Corporation, Bellefonte, PA, USA) packed column and a Thermal Conductivity Detector (TCD). The GC data was analyzed using PeakSimple software (SRI Instruments, Torrance, CA, USA) to calculate % by volume of methane and carbon dioxide.

The conversion of methane (v/v %) was calculated using the following equation:

$$\text{Conversion (v/v \%)} = \frac{[\text{CH}_4]_{\text{in}} - [\text{CH}_4]_{\text{out}}}{[\text{CH}_4]_{\text{in}}} \times 100\% \quad (1)$$

$[\text{CH}_4]_{\text{in}}$ = Volume % of methane at 1 atm and 25 °C in the gas feed entering the reactor.

$[\text{CH}_4]_{\text{out}}$ = Volume % methane at 1 atm and 25 °C in the gas mixture exiting the reactor.

For activity experiments, catalyst particle sizes of 63–75 μm , and gas flow rate of 150 cc/min at laboratory temperature of 25 °C and 1 atm were used. The GHSV was 45,000 cc.g.cat⁻¹.h⁻¹ at 25 °C and 1 atm. Activity runs were repeated and only runs with deviations below 2–3% were accepted. The gas feed composition was in volume % at 25 °C and 1 atm.

3.4. Effect of Steam

The effect of steam in the mixed gas feed was determined by passing a mixed gas (flow rate 150 cc/min) of 2% methane, 4% oxygen, and balance helium through a water bubbler. The percent of water vapor in the feed was 4.5%. The mixed gas (1.9% methane, 3.8% oxygen, 4.5% water vapor and

balance helium 1 atm and 25 °C) was passed through the catalyst bed separately at 350 °C and space velocity of 45,000 cc.g.cat⁻¹.h⁻¹ for a period of 2 and 4 h.

3.5. Stability Test of the Catalysts

The long term stability test of the catalysts were conducted in a fixed-bed catalytic reactor, A mixed gas feed (1% methane, 4% oxygen, balance helium) with a flow rate of 150 cc/min, GHSV of 45,000 cc.g.cat⁻¹.h⁻¹ at 25 °C and 1 atm., was passed over the catalyst bed at 350 °C. The effluent gas samples were drawn and analyzed in the GC at intervals of 24 h, 48 h and 72 h for both catalysts. The temperatures (T₂₅ and T₁₀₀) corresponding to 25% and 100% conversions were selected for the stability tests for each catalyst.

4. Conclusions

Pd/ γ -Al₂O₃ catalysts were synthesized by Vortex Method (VM) and Incipient Wetness Method (IWM) and characterized by various techniques (ICP-AES, Pulse CO Chemisorption, BET, TPR, XPS, XRD and STEM,) under identical conditions. From CO-pulse chemisorption, both catalysts had similar nanoparticle diameter (8.6–8.9 nm) and dispersions (12.6–13.1% Pd). XPS showed that surfaces of both catalysts contained PdO and PdO_x with about slightly more PdO_x in the 5-Pd-VM catalyst. HAADF-STEM images provided evidence for PdO/PdO_x nanocrystals (8–10 nm); the 5-Pd-VM catalyst had smaller nanoparticles and narrower particle size distribution compared to the 5-Pd-IWM catalyst. Although the 5-Pd-VM catalyst was more active in the lower temperature range of 275–325 °C, both catalysts achieved 100% conversion at 350 °C. The 5-Pd-VM catalyst displayed long-term stability and relative resistance to water deactivation. It is hypothesized that smaller metal nanoparticles with a narrower distribution and weaker PdO/PdO_x metal-support interaction may contribute to the higher activity in 5-Pd-VM catalyst.

Author Contributions: A.C.B. provided the concept and guidance for this research, contributed to data analysis and interpretation and much of the writing as the corresponding author; K.W.G. is co-first author based on her contributions: she contributed to characterization and interpretations, and also writing and editing of the manuscript; M.A.H. prepared the catalysts and did the activity studies; M.Z.B. did the XRD.

Funding: This research received no external funding.

Acknowledgments: This research was partly funded by Columbus State University Research Grants to A.B. and SRACE grants to M.A.H. Thanks to Yong Ding, Materials Characterization Facility at Georgia Institute of Technology for HAADF STEM and SEM imaging, particle size distribution and interpretations. This work was performed in part at the Georgia Tech Institute for Electronics and Nanotechnology, a member of the National Nanotechnology Coordinated Infrastructure, which is supported by the National Science Foundation (Grant ECCS-1542174).

Conflicts of Interest: The authors declare no conflict of interest.

References

1. Chen, J.; Arandiyana, H.; Gao, X.; Li, J. Recent Advances in Catalysts for Methane Combustion. *Catal. Surv. Asia* **2015**, *19*, 140–171. [[CrossRef](#)]
2. G elin, P.; Primet, M. Complete oxidation of methane at low temperature over noble metal based catalysts: A review. *Appl. Catal. B Environ.* **2002**, *39*, 1–37. [[CrossRef](#)]
3. Monai, M.; Montini, T.; Gorte, R.J.; Fornasiero, P. Catalytic Oxidation of Methane: Pd and Beyond. *Eur. J. Inorg. Chem.* **2018**, *2018*, 2884–2893. [[CrossRef](#)]
4. Banerjee, A.; McGuire, J.; Lawnick, O.; Bozack, M. Low-Temperature Activity and PdO-PdO_x Transition in Methane Combustion by a PdO-PdO_x/ γ -Al₂O₃ Catalyst. *Catalysts* **2018**, *8*, 266. [[CrossRef](#)]
5. Jiang, L.; Zheng, Y.; Chen, X.; Xiao, Y.; Cai, G.; Zheng, Y.; Zhang, Y.; Huang, F. Catalytic Activity and Stability over Nanorod-Like Ordered Mesoporous Phosphorus-Doped Alumina Supported Palladium Catalysts for Methane Combustion. *ACS Catal.* **2018**, *8*, 11016–11028.

6. Gorte, R.J.; Arroyo-Ramirez, L.; Chung, Y.-C.; Zhang, S.; Graham, G.W.; Onn, T.M.; Pan, X. Improved Thermal Stability and Methane-Oxidation Activity of Pd/Al₂O₃ Catalysts by Atomic Layer Deposition of ZrO₂. *ACS Catal.* **2015**, *5*, 5696–5701.
7. Goodman, E.D.; Dai, S.; Yang, A.C.; Wrasman, C.J.; Gallo, A.; Bare, S.R.; Hoffman, A.S.; Jaramillo, T.F.; Graham, G.W.; Pan, X.; et al. Uniform Pt/Pd Bimetallic Nanocrystals Demonstrate Platinum Effect on Palladium Methane Combustion Activity and Stability. *ACS Catal.* **2017**, *7*, 4372–4380. [[CrossRef](#)]
8. Simplício, L.M.T.; Brandão, S.T.; Sales, E.A.; Lietti, L.; Bozon-Verduraz, F. Methane combustion over PdO-alumina catalysts: The effect of palladium precursors. *Appl. Catal. B Environ.* **2006**, *63*, 9–14. [[CrossRef](#)]
9. Yoshida, H.; Nakajima, T.; Yazawa, Y.; Hattori, T. Support effect on methane combustion over palladium catalysts. *Appl. Catal. B Environ.* **2007**, *71*, 70–79. [[CrossRef](#)]
10. Liu, D.; Seeburg, D.; Kreft, S.; Bindig, R.; Hartmann, I.; Schneider, D.; Enke, D.; Wohlrab, S. Rice Husk Derived Porous Silica as Support for Pd and CeO₂ for Low Temperature Catalytic Methane Combustion. *Catalysts* **2019**, *9*, 26. [[CrossRef](#)]
11. Li, Y.; Luo, C.; Liu, Z.; Lin, F. Experimental Study on Catalytic Combustion of Methane in a Microcombustor with Metal Foam Monolithic Catalyst. *Catalysts* **2018**, *8*, 536. [[CrossRef](#)]
12. Cargnello, M.; Jaén, J.J.D.; Garrido, J.C.H.; Bakhmutsky, K.; Montini, T.; Gámez, J.J.C.; Gorte, R.J.; Fornasiero, P. Exceptional Activity for Methane Combustion over Modular Pd@CeO₂ Subunits on Functionalized Al₂O₃. *Science* **2012**, *337*, 713–718. [[CrossRef](#)] [[PubMed](#)]
13. Khader, M.; Al-Marri, M.; Ali, S.; Abdelmoneim, A. Active and Stable Methane Oxidation Nano-Catalyst with Highly-Ionized Palladium Species Prepared by Solution Combustion Synthesis. *Catalysts* **2018**, *8*, 66. [[CrossRef](#)]
14. Xiao, C.; Yang, Y.; Meng, D.; Dong, L.; Luo, L.; Tan, Z. Stable and active monolithic palladium catalyst for catalytic oxidation of methane using nanozeolite silicalite-1 coating on cordierite. *Appl. Catal. A Gen.* **2017**, *531*, 197–202. [[CrossRef](#)]
15. Li, M.; Gui, P.; Zheng, L.; Li, J.; Xue, G.; Liang, J. Active Component Migration and Catalytic Properties of Nitrogen Modified Composite Catalytic Materials. *Catalysts* **2018**, *8*, 125. [[CrossRef](#)]
16. Ercolino, G.; Stelmachowski, P.; Specchia, S. Catalytic Performance of Pd/Co₃O₄ on SiC and ZrO₂ Open Cell Foams for Process Intensification of Methane Combustion in Lean Conditions. *Ind. Eng. Chem. Res.* **2017**, *56*, 6625–6636. [[CrossRef](#)]
17. Zhang, X.; Long, E.; Li, Y.; Zhang, L.; Guo, J.; Gong, M.; Chen, Y. The effect of CeO₂ and BaO on Pd catalysts used for lean-burn natural gas vehicles. *J. Mol. Catal. A Chem.* **2009**, *308*, 73–78. [[CrossRef](#)]
18. Pantaleo, G.; Liotta, L.F.; Venezia, A.M.; Kantcheva, M.; Di Carlo, G. Effect of Ti(IV) loading on CH₄ oxidation activity and SO₂ tolerance of Pd catalysts supported on silica SBA-15 and HMS. *Appl. Catal. B Environ.* **2011**, *106*, 529–539.
19. Liotta, L.F.; Di Carlo, G.; Pantaleo, G.; Garrido, J.C.H.; Venezia, A.M. Pd (1 wt%)/LaMn_{0.4}Fe_{0.6}O₃ catalysts supported over silica SBA-15: Effect of perovskite loading and support morphology on methane oxidation activity and SO₂ tolerance. *Top. Catal.* **2012**, *55*, 782–791. [[CrossRef](#)]
20. Ma, J.; Lou, Y.; Cai, Y.; Zhao, Z.; Wang, L.; Zhan, W.; Guo, Y.; Guo, Y. The relationship between the chemical state of Pd species and the catalytic activity for methane combustion on Pd/CeO₂. *Catal. Sci. Technol.* **2018**, *8*, 2567–2577. [[CrossRef](#)]
21. Martin, A.; Liu, D.; Atia, H.; Schneider, M.; Wohlrab, S.; Pohl, M.-M.; Radnik, J.; Seeburg, D. Structural Changes of Highly Active Pd/MeOx (Me = Fe, Co, Ni) during Catalytic Methane Combustion. *Catalysts* **2018**, *8*, 42.
22. Lundgren, E.; Nilsson, J.; Gustafson, J.; Grönbeck, H.; Skoglundh, M.; Newton, M.A.; Fouladvand, S.; Carlsson, P.-A.; Martin, N.M. Chemistry of Supported Palladium Nanoparticles during Methane Oxidation. *ACS Catal.* **2015**, *5*, 2481–2489.
23. Miller, J.B.; Malatpure, M. Pd catalysts for total oxidation of methane: Support effects. *Appl. Catal. A Gen.* **2015**, *495*, 54–62. [[CrossRef](#)]
24. Christ, B.V. *Handbook of Monochromatic Xps Spectra. The Elements of Native Oxides*; Wiley-VCH: Weinheim, Germany, 2000; p. 49265. ISBN 0-471-49265-5.
25. Gil, S.; Retailleau, L.; Garcia-Vargas, J.; Ousmane, M.; Pantaleo, G.; Giroir-Fendler, A.; Liotta, L. Catalytic Oxidation of Propene over Pd Catalysts Supported on CeO₂, TiO₂, Al₂O₃ and M/Al₂O₃ Oxides (M = Ce, Ti, Fe, Mn). *Catalysts* **2015**, *5*, 671–689. [[CrossRef](#)]

26. Sadokhina, N.; Ghasempour, F.; Auvray, X.; Smedler, G.; Nylén, U.; Olofsson, M.; Olsson, L. An Experimental and Kinetic Modelling Study for Methane Oxidation over Pd-based Catalyst: Inhibition by Water. *Catal. Lett.* **2017**, *147*, 2360–2371. [[CrossRef](#)]
27. Bychkov, V.Y.; Tyulenin, Y.P.; Gorenberg, A.Y.; Sokolov, S.; Korchak, V.N. Evolution of Pd catalyst structure and activity during catalytic oxidation of methane and ethane. *Appl. Catal. A Gen.* **2014**, *485*, 1–9. [[CrossRef](#)]
28. Xiong, H.; Wiebenga, M.H.; Carrillo, C.; Gaudet, J.R.; Pham, H.N.; Kunwar, D.; Oh, S.H.; Qi, G.; Kim, C.H.; Datye, A.K. Design considerations for low-temperature hydrocarbon oxidation reactions on Pd based catalysts. *Appl. Catal. B Environ.* **2018**, *236*, 436–444. [[CrossRef](#)]
29. Schwartz, W.R.; Pfefferle, L.D. Combustion of methane over palladium-based catalysts: Support interactions. *J. Phys. Chem. C* **2012**, *116*, 8571–8578. [[CrossRef](#)]
30. Di, L.; Xu, W.; Zhan, Z.; Zhang, X. Synthesis of alumina supported Pd-Cu alloy nanoparticles for CO oxidation via a fast and facile method. *RSC Adv.* **2015**, *5*, 71854–71858. [[CrossRef](#)]
31. Ercolino, G.; Karimi, S.; Stelmachowski, P.; Specchia, S. Catalytic combustion of residual methane on alumina monoliths and open cell foams coated with Pd/Co₃O₄. *Chem. Eng. J.* **2017**, *326*, 339–349. [[CrossRef](#)]
32. Van Giezen, J.C.; Van Den Berg, F.R.; Kleinen, J.L.; Van Dillen, A.J.; Geus, J.W. The effect of water on the activity of supported palladium catalysts in the catalytic combustion of methane. *Catal. Today* **1999**, *47*, 287–293. [[CrossRef](#)]
33. Stefanov, P.; Todorova, S.; Naydenov, A.; Tzaneva, B.; Kolev, H.; Atanasova, G.; Stoyanova, D.; Karakirova, Y.; Aleksieva, K. On the development of active and stable Pd-Co/ γ -Al₂O₃ catalyst for complete oxidation of methane. *Chem. Eng. J.* **2015**, *266*, 329–338. [[CrossRef](#)]
34. Ercolino, G.; Stelmachowski, P.; Grzybek, G.; Kotarba, A.; Specchia, S. Optimization of Pd catalysts supported on Co₃O₄ for low-temperature lean combustion of residual methane. *Appl. Catal. B Environ.* **2017**, *206*, 712–725. [[CrossRef](#)]
35. Burch, R.; Urbano, F.J.; Loader, P.K. Methane combustion over palladium catalysts: The effect of carbon dioxide and water on activity. *Appl. Catal. A Gen.* **1995**, *123*, 173–184. [[CrossRef](#)]
36. Ciuparu, D.; Pfefferle, L. Support and water effects on palladium based methane combustion catalysts. *Appl. Catal. A Gen.* **2001**, *209*, 415–428. [[CrossRef](#)]
37. Persson, K.; Pfefferle, L.D.; Schwartz, W.; Ersson, A.; Järås, S.G. Stability of palladium-based catalysts during catalytic combustion of methane: The influence of water. *Appl. Catal. B Environ.* **2007**, *74*, 242–250. [[CrossRef](#)]
38. Huang, F.; Chen, J.; Hu, W.; Li, G.; Wu, Y.; Yuan, S.; Zhong, L.; Chen, Y. Pd or PdO: Catalytic active site of methane oxidation operated close to stoichiometric air-to-fuel for natural gas vehicles. *Appl. Catal. B Environ.* **2017**, *219*, 73–81. [[CrossRef](#)]
39. Forzatti, P. Status and perspectives of catalytic combustion for gas turbines. *Catal. Today* **2003**, *83*, 3–18. [[CrossRef](#)]
40. Gholami, R.; Smith, K.J. Activity of PdO/SiO₂ catalysts for CH₄ oxidation following thermal treatments. *Appl. Catal. B Environ.* **2015**, *168–169*, 156–163. [[CrossRef](#)]
41. Sulmonetti, T.P.; Pang, S.H.; Claire, M.T.; Lee, S.; Cullen, D.A.; Agrawal, P.K.; Jones, C.W. Vapor phase hydrogenation of furfural over nickel mixed metal oxide catalysts derived from layered double hydroxides. *Appl. Catal. A Gen.* **2016**, *517*, 187–195. [[CrossRef](#)]
42. Walton, K.S.; Snurr, R.Q. Applicability of the BET method for determining surface areas of microporous metal-organic frameworks. *J. Am. Chem. Soc.* **2007**, *129*, 8552–8556. [[CrossRef](#)]

